Performance Evaluation of Wavelet Transform Application in Maximum-Rank-Distance-Based STBC-OFDM System

Arslan Khalid, *Student Member*; *IEEE*, Prapun Suksompong, and Chalie Charoenlarpnopparut
School of Information, Computer and Communication Technology,
Sirindhorn International Institute of Technology, Thammasat University
engr.arslan08@gmail.com, {prapun,chalie}@siit.tu.ac.th

***Abstract*—Integrating space-time block coding (STBC) with orthogonal frequency division multiplexing (OFDM) has become a promising wireless communications solution that provides high data transmission rates and improved signal quality. Conventional (orthogonal and non-orthogonal) STBCs had a tradeoff between transmission rates and maximum diversity when applied in STBC-OFDM systems with more than two transmit antenna chains. The Fourier transform-based OFDM also has a high peak-to-average power ratio (PAPR) that deteriorates system performance. This work addresses the mentioned issues using wavelet-transform-based OFDM (WOFDM) and STBCs based on maximum-rank-distance (MRD) codes, i.e., MRD-STBCs. In the proposed MRD-STBC-WOFDM system, MRD-STBCs provide rate-1 transmissions with maximum diversity, while WOFDM enhances bit-error-rate (BER) and PAPR performance. Compared with conventional STBC-OFDM, the proposed system with three transmit antennas has significant BER and PAPR improvement. Moreover, the wavelet transform application in MRD-STBC-OFDM reduces the OFDM's complexity.**

***Index Terms*—Bit-error-rate (BER), Finite field, Maximum-rank-distance (MRD) codes, OFDM, Space-time block coding (STBC)**

I. Introduction

Communication technology has undergone global transformations over two decades, leading to a massive upsurge in using wireless technology as the prime communication mode. The fundamental objective in designing a wireless communication system is to deliver high transmission rate wireless multimedia content by guaranteeing service quality over the diverse wireless fading channels. Multiple input multiple output (MIMO) technology, employing multiple transmitter and receiver antennas, is the most distinguished technology that effectively addressed the afore-given objective using several independent data pipelines resulting from antenna diversity [1].

MIMO technology has been extensively implemented with the space-time block coding (STBC) technique. Alamouti in [2] initially devised an elegant orthogonal STBC (OSTBC) framework for two-antenna configurations. The key advantage of it was the utilization of orthogonal columns of the code matrix that helped it to achieve maximum diversity with rate-1 transmissions at very low computational maximum likelihood (ML) decoding complexity. Following Alamouti's proposal, Tarokh established an orthogonal design theory for OSTBC construction [3]. According to it, OSTBCs designed over complex constellations possessed maximum diversity, while the unity rate vanished when applied with more than two transmit antennas.

Many information theorists subsequently developed non-orthogonal STBCs (NOSTBCs) by compromising orthogonality conditions in code design [4]–[6]. They achieved rate-1 transmissions while having an exponential increase in ML decoding complexity. Remarkably, the relaxation in the code's orthogonality also diminished their maximum diversity. An exciting class of NOSTBCs came into existence from the efforts of Gabidulin, who constructed them using maximum-rank-distance (MRD) codes, i.e., MRD-STBCs [7]. Opposite to other NOSTBCs, MRD-STBCs retained maximum diversity and provided rate-1 transmissions for arbitrary transmit antenna chains.

STBC-based MIMO technology integrated with multi-carrier orthogonal frequency division multiplexing (OFDM) promised high data transmission rates by combating signal fading over wireless channels [8]. This proposal led to its inclusion in Third Generation Partnership Projects (3GPP) [9] and IEEE standard families for wireless local area networks (WLAN, IEEE 802.11) [10] and metropolitan area networks (MAN, IEEE 802.16) [11]. However, the non-unity rate issue of OSTBCs, when applied with more than two transmit antennas, restricted the transmission rates achievable through the OSTBC-OFDM system. Recently, we addressed this issue by proposing an MRD-STBC-OFDM system that increases the data transmission rates in cases with more than two transmit antennas [12].

The proposed system used OFDM as a waveform technique. It had a high peak-to-average power ratio (PAPR) and a non-compact sinc-shaped spectrum [13]. In the literature, numerous multi-carrier waveforms, such as filter bank multi-carrier (FBMC) [14], generalized frequency division multiplexing (GFDM) [15], universal filtered multi-carrier (UFMC) [16], and wavelet-transform-based OFDM (WOFDM) [17] were proposed that widely combated OFDM issues for single-antenna communications.

For MIMO systems, the authors of [18] first integrated Alamouti STBC with the FBMC waveform. BER and PAPR outcomes revealed that the STBC-FBMC-based MIMO system performance was worse than the Alamouti-based STBC-OFDM. The intrinsic self-interference of FBMC caused this performance deterioration. Cheema et al. [19] studied the overall performance of Alamouti-based STBC-UFMC and STBC-GFDM systems and compared them with conventional Alamouti STBC-OFDM. Simulated results showed the BER performance of STBC-UFMC and STBC-GFDM could not beat Alamouti STBC-OFDM but remained close to it.

979-8-3503-0219-6/23/$31.00 ©2023 IEEE

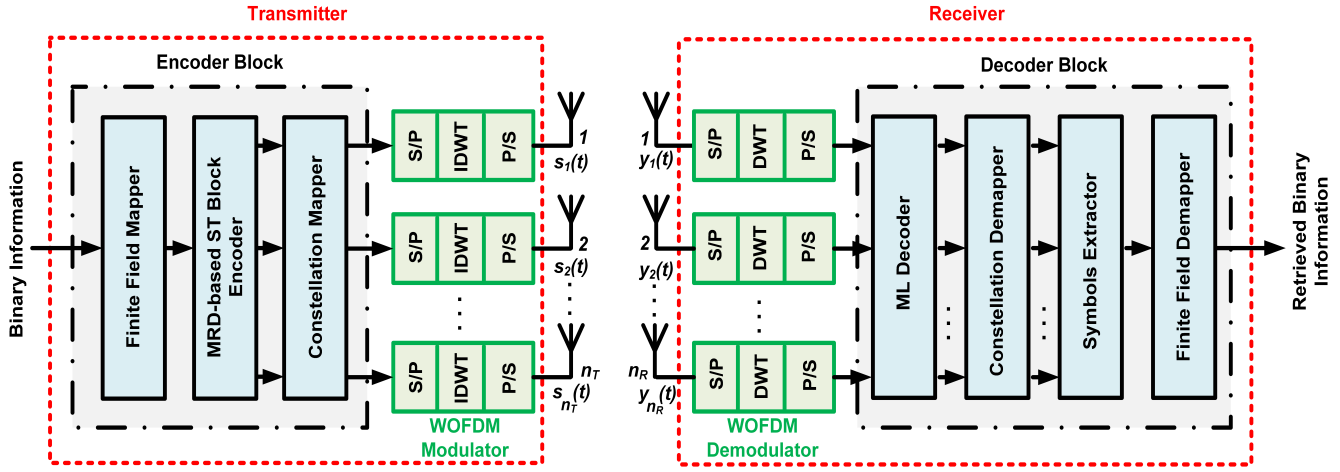

Fig. 1. Proposed MRD-STBC-WOFDM system model.

To the best of the authors' knowledge, few works are available that implemented the STBC-OFDM system using wavelet transform, i.e., STBC-WOFDM [20]–[22]. The BER results in these works showed that STBC-WOFDM outperforms conventional STBC-OFDM systems. However, the PAPR performance and computational complexity of STBC-WOFDM are still unexplored. In particular, no previously published work presented an MRD-STBC-WOFDM system proposal. This paper extends our earlier work [12] and targets its performance improvement. Its core contribution is to apply wavelet transform application in an MRD-STBC-OFDM system and explore its performance.

The paper structure is based on the following sections. Section II dedicates to the proposed MRD-STBC-WOFDM system model, while Section III briefly discusses the direct matrix MRD-STBC construction method, followed by an example. The presented method generates a full rank rate-1 MRD-STBC codebook for any number of transmitting antennas. Section IV will explain the simulation setup. It will also display the BER and PAPR outcomes for 2×2 and 3×3 MIMO configurations and discusses the proposed system complexity. Section V of the paper will derive conclusions.

II. SYSTEM MODEL

This section elaborates on the proposed MRD-STBC-WOFDM system model developed using the standard implementation of the MRD-STBC-OFDM system presented in our earlier work [12]. The reader must review it thoroughly to understand better the working of each block used in the proposed system model. Here, we will briefly describe each block and primarily focus on integrating inverse discrete wavelet transform (IDWT) and DWT operations within the MRD-STBC system. Fig. 1 illustrates the MIMO wireless WOFDM system that uses the MRD-STBC framework with n_T and n_R transmitting and receiving antennas, respectively. A binary source forwards information bits to the encoder block of the transmitter that processes it through a finite field mapper, an MRD-based space-time (ST) block encoder, and a constellation mapper.

The finite field mapper maps the information bits onto algebraic symbols in a finite field. Afterward, an MRD-based ST block encoder breaks them into $n_T \times 1$ vectors and maps each vector on an MRD-STBC codeword. Without compromising generality, the MRD-STBC scheme considers information symbols in the matrix codeword's first column. After encoding, the ST block encoder concatenates the matrix codewords to form the signals. It passes them to the constellation mapper that uses quadrature amplitude modulation (QAM) to map each entry on the complex constellation point.

The encoder block individually supplies each complex output signal to the WOFDM modulator block that first breaks it into low-rate parallel, closely spaced orthogonal frequency sub-carriers by employing a serial-to-parallel (S/P) block. Subsequently, the IDWT block receives these sub-carriers and processes them using a synthesis filter-bank [23]. It decomposes the frequency-domain sub-carriers and changes them into time-domain WOFDM symbols. As a prototype filter, the IDWT block works with different wavelet filter families, from which Haar, Meyer, Symlets, Daubechies, and Biorthogonal are a few names to mention. Inside the block, the input sub-carrier S_c spectrum splits into approximate/scaling and detail information using successive low-pass $a[n]$ and high-pass $d[n]$ filters. Mathematically, one can write the outcome of the IDWT block using [24]

$$\begin{aligned} s_c = &\sqrt{2^{-(l-1)}} \sum_{l\in I} O_l^0 \phi(2^{-(l-1)}t - l) \\ &+ \sum_{m=1}^{l-1} \sqrt{2^{-(l-m)}} \sum_{l\in I} O_l^m \psi(2^{-(l-m)}t - l). \end{aligned} \tag{1}$$

Here, l signifies the decomposition level, O_l^m shows the modulated symbols having $m = 0, 1, 2, \ldots, l-1$, I is the integer used for indexing, $\phi(t)$ and $\psi(t)$ are the scaling and detailed functions, respectively. These functions are [24]:

$$\begin{aligned} \phi(t) &= \sqrt{2} \sum_{n\in I} a[n]\phi(2t - n), \\ \psi(t) &= \sqrt{2} \sum_{n\in I} d[n]\psi(2t - n). \end{aligned} \tag{2}$$

After performing the IDWT operation, the cyclic prefix is unnecessary for the proposed system, as wavelets have intrinsic time and frequency localization capability [17]. The

parallel-to-serial (P/S) block combines WOFDM symbols to create a frame for transmission. Similarly, other WOFDM blocks also produce frames $s_i(t)$, (where $i = 1, 2, \ldots, n_T$), and the transmitter uses active antennas to send them towards the receiver over a free-space MIMO channel. While traveling from transmitter to receiver, each frame undergoes quasi-static Rayleigh fading that follows a complex Gaussian distribution with zero mean and unit variance. The response of such fading remains static for the complete WOFDM frame transmission and varies from frame to frame [3].

Each antenna on the receiver received a mixture of transmitted frames, perturbed by complex Gaussian distributed noise. The receiver treats each received frame $y_j(t)$ (where $j = 1, 2, \ldots, n_R$) by breaking it into parallel symbols using the S/P block. DWT block uses the analysis filter-bank $a[-n]$ and $d[-n]$ to denoise and transform them into the frequency domain sub-carriers. The following relations represent the DWT working [24]:

$$\begin{aligned} \phi_{2^l} &= \sum_{l \in I} a[l - 2n]\ y_j(t), \\ \psi_{2^l} &= \sum_{l \in I} d[l - 2n]\ y_j(t). \end{aligned} \tag{3}$$

In the last step of the WOFDM demodulator, the P/S block forms high-rate signals from the DWT-processed sub-carriers and forwards them to a decoder block. Inside it, the ML decoder disintegrates the received MRD-STBC signals into $n_T \times n_T$ matrix codewords and uses the channel knowledge to determine the transmitted matrix codewords [12]. Decoded codewords then apply to the constellation demapper block that maps each constellation point back to the finite field symbol. Afterward, the symbols extractor block extracts the information symbols from the matrix codeword's first column and combines them to form a serial symbol stream. The final stage of the decoder uses the finite field demapper that converts the finite field symbols back to the bit stream.

III. MRD-STBC CONSTRUCTION

Typically, MRD-STBCs for any arbitrary number of transmit antenna chains are constructed using a direct matrix-based approach [7]. This approach requires the n_T-degree primitive polynomial coefficients and generate a codebook with distinct $n_T \times n_T$ matrix codewords. Let a generalized n_T-degree primitive polynomial is

$$g(x) = x^{n_T} + c_{n_T-1}.x^{n_T-1} + c_{n_T-2}.x^{n_T-2} + \ldots + c_1.x + c_0, \tag{4}$$

and its coefficients are finite (Galois) field elements, i.e., GF$(q) = \{0, 1, 2, \ldots, q-1\}$. The direct matrix approach uses these coefficients and produces the codebook as:

$$\mathbf{M}^k = \begin{bmatrix} 0 & 0 & \cdots & 0 & -c_0 \\ 1 & 0 & \cdots & 0 & -c_1 \\ 0 & 1 & \cdots & 0 & -c_2 \\ \vdots & \vdots & \ddots & \vdots & \vdots \\ 0 & 0 & \cdots & 0 & -c_{n_T-2} \\ 0 & 0 & \cdots & 1 & -c_{n_T-1} \end{bmatrix}^k, \ 1 \le k \le q^{n_T} - 1. \tag{5}$$

Adding a zero matrix (a possible matrix codeword) in the codebook completes the code construction. MRD-based ST block encoder in Section II requires the information symbols to be available in the matrix codeword's first column. The code validity conditions presented in [12] ensure this feature. According to these conditions, an MRD-STBC should not have the same symbol combination in the first column of two matrix codewords, and it should cover all potential symbol combinations that can be formed using the symbols available within the selected symbol space. A code that fulfills the given criteria is valid and suitable for transmission. Each $n_T \times n_T$ matrix codeword in the codebook has a rank equal to n_T. Before transmission, these codewords over GF(q) must transform into a collection of full-rank $n_T \times n_T$ matrix codewords over the complex field using rank-preserving mappings [25], such as PSK or QAM. In what follows next, a construction example for $n_T = 2$ and $q = 2^2$ is available to clarify the construction procedure.

Example: The construction procedure employs a finite binary extension field $q = 2^2$. According to field order and n_T, the codebook cardinality is $q^{n_T} = (2^2)^2 = 16$. For finite binary fields, a second-degree extension field primitive polynomial is $x^2 + c_1 x + c_0$. The coefficients of this polynomial are from GF$\left(2^2\right) = \left\{0, 1, \alpha, \alpha^2\right\}$. Let the coefficients of the second-degree polynomial be $c_1 = \alpha^2$ and $c_0 = \alpha^2$ and according to (4), the polynomial becomes $x^2 + \alpha^2 x + \alpha^2$. From these coefficients, the direct matrix approach using (5) generates a codebook with the following rank-2 matrix codewords

$$\begin{aligned} &\mathbf{M}^1 = \begin{bmatrix} 0 & \alpha^2 \\ 1 & \alpha^2 \end{bmatrix} \quad \mathbf{M}^2 = \begin{bmatrix} \alpha^2 & \alpha \\ \alpha^2 & 1 \end{bmatrix} \quad \mathbf{M}^3 = \begin{bmatrix} \alpha & \alpha^2 \\ 1 & 1 \end{bmatrix} \\ &\qquad\vdots \qquad\qquad\qquad\vdots \qquad\qquad\qquad\vdots \\ &\mathbf{M}^{13} = \begin{bmatrix} \alpha^2 & 1 \\ \alpha & \alpha \end{bmatrix} \quad \mathbf{M}^{14} = \begin{bmatrix} 1 & 1 \\ \alpha & 0 \end{bmatrix} \quad \mathbf{M}^{15} = \begin{bmatrix} 1 & 0 \\ 0 & 1 \end{bmatrix} \end{aligned} \tag{6}$$

A zero matrix is included in the above collection of matrix codewords to complete the codebook. Upon analyzing the codebook, it becomes evident that each matrix codeword transmits two information symbols over two-time slots. This attribute signifies that MRD-STBC has the capability of rate-1 transmission.

IV. SIMULATION RESULTS AND DISCUSSIONS

This section evaluates the overall performance of the proposed MRD-STBC-WOFDM system by benchmarking BER, PAPR, and computational complexity metrics. The performance is compared with some known conventional orthogonal and non-orthogonal STBC-OFDM systems. We developed the computer programs for 2×2 and 3×3 MIMO antenna configurations. An OFDM frame has 256 data sub-carriers that carry 4-QAM complex symbols. The Fourier transform-based OFDM uses a rectangular filter as a prototype filter, while WOFDM exploits the Haar wavelet owing to its best performance compared to other wavelet families [26].

Before physical transmission, the simulation programs normalize the average energy of the signals sent from each antenna. All proposed and conventional STBC-OFDM systems are simulated under quasi-static Rayleigh fading and

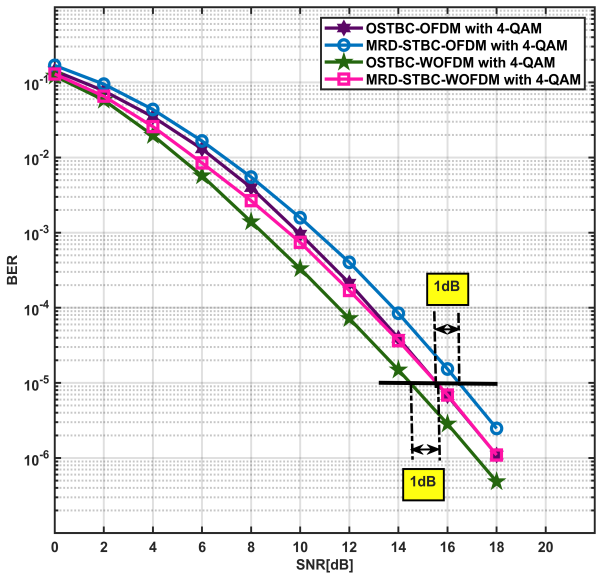

Fig. 2. BER performance comparison of proposed MRD-STBC-WOFDM and conventional Alamouti-based STBC-OFDM systems for 2×2 antenna configuration.

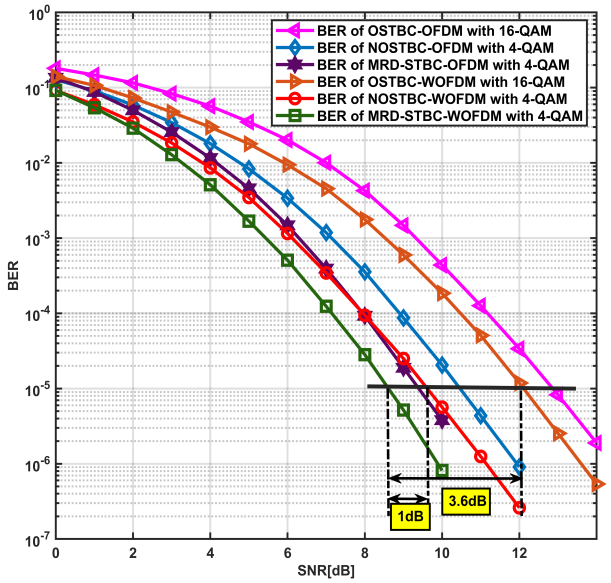

Fig. 3. BER performance comparison of proposed MRD-STBC-WOFDM and conventional OSTBC- and NOSTBC-OFDM systems for 3×3 antenna configuration.

follow two assumptions: 1) the transmitter-receiver pair is in perfect time and frequency synchronization, and 2) the receiver knows the exact channel information. Monte Carlo simulations find the BER against the SNR values ranging from 0 to 18dB by averaging over the repetition of 10^6 OFDM frames.

A. BER Comparisons

Fig. 2 exhibits BER results for 2×2 antenna configurations. Here, the conventional STBC-OFDM system uses the famous Alamouti code [2], which we call OSTBC-OFDM. Our proposed system used MRD-STBC constructed over GF(2^2), available as a construction example in Section III. The simulations for both Fourier transform OSTBC- and MRD-STBC-OFDM are also conducted for performance assessment. Analysis of BER curves reveals that at 10^{-5} BER, the MRD-STBC-OFDM system, due to non-orthogonality, demonstrates 1dB less coding gain than OSTBC-OFDM. However, this coding gap is reduced by replacing Fourier transform OFDM with wavelet OFDM. The proposed MRD-STBC-WOFDM system benefits from wavelets' time and frequency localization capability and, at high SNR values, has comparable performance to OSTBC-OFDM. At the same time, if a conventional system uses WOFDM, its performance is again 1dB better than the proposed one. Here, one could not observe the proposed system's main benefit because, for 2×2 antenna configurations, Alamouti code and MRD-STBC provide rate-1 transmissions. The benefits of our proposed technique will be evident through 3×3 antenna configurations, where MRD-STBC has a unity code rate compared to OSTBC.

Fig. 3 illustrates the BER outcomes of 3×3 antenna configurations, aligning with our objective of achieving maximum diversity with rate-1 transmissions. Firstly, note that OSTBCs are available with half- or three-quarters rates for three transmit antennas [3]. By employing high constellation cardinality, these OSTBCs achieve transmission rates similar to those obtained by the proposed system. For instance, the MRD-STBC with 4-QAM has a transmission rate of 2 bits per time slot. Achieving the same transmission rate using the half-rate OSTBC given by Tarokh (see (37) in [3]) requires 16-QAM. Our computer programs adopted this setting to develop the OSTBC-OFDM system. Since MRD-STBCs belong to a class of NOSTBCs, comparing their performance with known corresponding NOSTBCs is more appropriate. For this, computer programs also used the code matrix introduced by Uysal (see (6) given in [6]).

For the proposed system, an MRD-STBC over GF(2^2) is constructed using a third-degree polynomial $g(x) = x^3 + c_2x^2 + c_1x + c_0$. The coefficients for the considered polynomial are $c_2 = c_1 = c_0 = \alpha$. The codebook is generated with $q^{n_T} = 64$ matrix codewords using (5). The finite field entries of the matrix codewords map to the complex plane using 4-QAM. All systems are simulated, and their BER outcomes are compared in Fig. 3. At 10^{-5} BER, it is apparent that MRD-STBC-OFDM outperforms the conventional OSTBC- and NOSTBC-OFDM systems. Compared with OSTBC-OFDM, the MRD-STBC-OFDM has a coding gain of 3.6dB, while this gain narrowed down to approximately 1dB for NOSTBC-OFDM. The performance degradation observed in OSTBC-OFDM can be traced back to the attempt to fix the transmission rates of half-rate OSTBC using high constellation cardinality. The diversity order of NOSTBC-OFDM is less than MRD-STBC-OFDM system [12]. Therefore, it requires more SNR to compensate for the detrimental channel effects. Using WOFDM in all systems also improves their error performances. However, WOFDM could not provide the ability to OSTBC- and NOSTBC-OFDM systems such that they can beat our proposed MRD-STBC-WOFDM system.

B. PAPR Comparisons

This section draws attention to another vital performance index called PAPR. Typically OFDM-based systems use Fourier transforms to process the N low-rate sub-carriers. These sub-carriers join together and cause high PAPR values. Consequently, the high-power amplifier operates in the non-linear region, causing intermodulation distortion in the system. More specifically, PAPR is the ratio of instantaneous peak power P_{peak} to the signal's average power P_{avg} given as [24]:

$$\text{PAPR} = \frac{P_{peak}}{P_{avg}} = \frac{max\left[|s(n)|^2\right]}{E\left[|s(n)|^2\right]} \quad for \quad 0 \leq n \leq (N.L-1) \tag{7}$$

where $E[\cdot]$ shows the expected signal value and L is an oversampling factor. A discrete signal $s(n)$ does not hold all signal peaks of a continuous signal $s(t)$. Therefore, the PAPR of $s(n)$ differs from the PAPR of $s(t)$. An oversampling factor has been introduced in the system to remove this difference. According to [24], [26], $L = 4$ is sufficient to compare the PAPR of a discrete signal with the continuous one. The statistical properties of PAPR of an OFDM waveform having N sub-carriers are characterized by its complementary cumulative distribution function (CCDF). It shows how much the PAPR of OFDM surpasses a given threshold value ξ, i.e., [24], [26]

$$\text{CCDF}\left(N, \xi\right) = P_r\left\{\text{PAPR} > \xi\right\} = 1 - \left(1 - e^{-\xi}\right)^N. \tag{8}$$

In MIMO-based OFDM systems, one can evaluate PAPR by finding the maximum PAPR value among all PAPR values of simultaneously transmitting antennas. For PAPR analysis, Fig. 4 only presents the results of the conventional and proposed STBC-OFDM systems for 2×2 antenna configurations. The results of 3×3 case follow similar patterns. Each system transmits 10^6 OFDM frames with $N = 256$ and $L = 4$. Two key observations are deduced from the PAPR outcomes presented in Fig. 4. Firstly, the PAPR profile of the MRD-STBC-OFDM system overlaps with the conventional OSTBC-OFDM system, showing that it operates at the same power as the conventional one. Secondly, the proposed MRD-STBC-WOFDM has superior PAPR performance than the MRD-STBC-OFDM. At 10^{-5} CCDF, the PAPR profiles of the MRD-STBC-WOFDM system attain a 4dB gain, which is realized without employing any PAPR reduction technique. One could also observe the similarity in PAPR profiles of MRD-STBC-WOFDM and OSTBC-WOFDM.

C. Complexity Comparisons

Having shown the improved BER and PAPR performance of the proposed MRD-STBC-WOFDM system, this paper also sheds light on its computational complexity. The OFDM block in the MRD-STBC-OFDM system uses a fast Fourier transform. It has a computational complexity of $\mathcal{O}(N.\log N)$ in terms of additions and multiplications [27]. WOFDM, with the use of multi-resolution DWT, reduces this complexity to $\mathcal{O}(N)$, under the condition that the wavelet's filter length is negligible in comparison to N [24], [26].

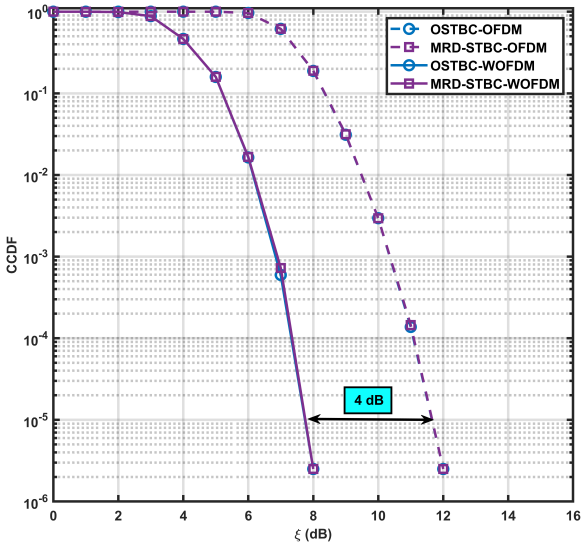

Fig. 4. PAPR profiles of proposed and conventional STBC-OFDM systems.

In the meantime, the receiver uses a brute-force ML decoder that completes its search for the transmitted matrix codeword in $\mathcal{O}(q^m)^{n_T}$ computations. The conventional MRD-STBC-OFDM system also employs it and therefore has the same complexity as a wavelet-based system. Our complexity calculations concluded that the proposed MRD-STBC-WOFDM system has the additional advantage of being less computationally complex than our earlier proposed system in [12].

V. Concluding Remarks

This paper integrated the framework of MRD-STBC with a wavelet-based OFDM waveform and studied its behavior using BER, PAPR, and computational complexity as performance metrics. In the proposed MRD-STBC-WOFDM system, MRD-STBCs fix the code rate and maximum diversity issues of conventional STBCs, while WOFDM combats OFDM problems. Compared to the Alamouti-based OSTBC-WOFDM system, our non-orthogonal system has 1dB performance deterioration. However, it shows considerable BER performance improvements (as depicted in Fig. 3) against the OSTBC- and NOSTBC-OFDM systems for three transmit antennas. The PAPR profile of the MRD-STBC-WOFDM system has outperformed the conventional MRD-STBC-OFDM system and achieved a gain of 4dB without additional PAPR reduction techniques. Moreover, the proposed system reduces the OFDM's complexity compared to our conventional MRD-STBC-OFDM system. For future work, one may investigate the performance of the proposed system under different channel models or concatenate the MRD-STBCs with the capacity-approaching channel coding schemes to attain more coding gains.

Acknowledgment

This research is supported by the Excellent Foreign Student scholarship program, Sirindhorn International Institute of Technology.

REFERENCES

[1] E. Telatar, "Capacity of multi-antenna gaussian channels," *European Transactions on Telecommunications*, vol. 10, no. 6, pp. 585–595, 1999.

[2] S. M. Alamouti, "A simple transmit diversity technique for wireless communications," *IEEE Journal on Selected Areas in Communications*, vol. 16, no. 8, pp. 1451–1458, 1998.

[3] V. Tarokh, H. Jafarkhani, and A. R. Calderbank, "Space-time block codes from orthogonal designs," *IEEE Transactions on Information Theory*, vol. 45, no. 5, pp. 1456–1467, 1999.

[4] H. Jafarkhani, "A quasi-orthogonal space-time block code," *IEEE Transactions on Communications*, vol. 49, no. 1, pp. 1–4, 2001.

[5] C. B. Papadias and G. J. Foschini, "Capacity-approaching space-time codes for systems employing four transmitter antennas," *IEEE Transactions on Information Theory*, vol. 49, no. 3, pp. 726–732, 2003.

[6] M. Uysal and C. Georghiades, "Non-orthogonal space-time block codes for 3Tx antennas," *Electronics Letters*, vol. 38, no. 25, p. 1, 2002.

[7] E. M. Gabidulin, M. Bossert, and P. Lusina, "Space-time codes based on rank codes," in *IEEE International Symposium on Information Theory (Cat. No. 00CH37060)*. IEEE, 2000, p. 284.

[8] K. Lee and D. Williams, "A space-time coded transmitter diversity technique for frequency selective fading channels," in *Proceedings of the 2000 IEEE Sensor Array and Multichannel Signal Processing Workshop. SAM 2000 (Cat. No.00EX410)*, 2000, pp. 149–152.

[9] N. P. S. Andersen, "The third generation partnership project (3GPP)," *GSM and UMTS*, vol. 247, 2001.

[10] "IEEE standard for information technology– local and metropolitan area networks– specific requirements– part 11: Wireless LAN medium access control (MAC) and physical layer (PHY) specifications amendment 5: Enhancements for higher throughput," *IEEE Std 802.11n-2009 (Amendment to IEEE Std 802.11-2007 as amended by IEEE Std 802.11k-2008, IEEE Std 802.11r-2008, IEEE Std 802.11y-2008, and IEEE Std 802.11w-2009)*, pp. 1–565, 2009.

[11] "IEEE standard for local and metropolitan area networks - part 16: Air interface for fixed and mobile broadband wireless access systems - amendment for physical and medium access control layers for combined fixed and mobile operation in licensed bands," *IEEE Std 802.16e-2005 and IEEE Std 802.16-2004/Cor 1-2005 (Amendment and Corrigendum to IEEE Std 802.16-2004)*, pp. 1–822, 2006.

[12] A. Khalid and P. Suksompong, "Application of maximum rank distance codes in designing of STBC-OFDM system for next-generation wireless communications," *Digital Communications and Networks*, 2023. [Online]. Available: https://doi.org/10.1016/j.dcan.2022.12.022

[13] R. Saxena and H. D. Joshi, "OFDM and its major concerns: a study with way out," *IETE Journal of Education*, vol. 54, no. 1, pp. 26–49, 2013.

[14] B. Farhang-Boroujeny, "Filter bank multicarrier modulation: A waveform candidate for 5G and beyond," *Advances in Electrical Engineering*, vol. 2014, 2014.

[15] A. K. Permana and E. Y. Hamid, "Performance evaluation of GFDM channel estimation using DFT for tactile internet application," *Electronics*, vol. 10, no. 5, p. 595, 2021.

[16] I. Baig, U. Farooq, N. U. Hasan, M. Zghaibeh, and V. Jeoti, "A multicarrier waveform design for 5G and beyond communication systems," *Mathematics*, vol. 8, no. 9, p. 1466, 2020.

[17] M. Ghanim, "Performance investigation of WOFDM for 5G wireless networks," *International Journal of Electrical and Computer Engineering*, vol. 9, no. 4, p. 3153, 2019.

[18] R. Zakaria and D. Le Ruyet, "A novel filter-bank multicarrier scheme to mitigate the intrinsic interference: Application to MIMO systems," *IEEE Transactions on Wireless Communications*, vol. 11, no. 3, pp. 1112–1123, 2012.

[19] S. A. Cheema, K. Naskovska, M. Attar, B. Zafar, and M. Haardt, "Performance comparison of space time block codes for different 5G air interface proposals," in 20^{th} *International ITG Workshop on Smart Antennas*. VDE, 2016, pp. 1–7.

[20] S. Q. Hadi, P. Ehkan, M. Anuar, and A. A. Jafaar, "STBC-OFDM system based on discrete framelet transform," *Journal of Theoretical and Applied Information Technology*, vol. 84, no. 2, p. 250, 2016.

[21] N. Parveen, K. Abdullah, R. Islam, and R. I. Boby, "Diversity technique using discrete wavelet transform in OFDM system," *International Journal of Engineering and Advanced Technology (IJEAT) ISSN*, vol. 2249, no. 1, pp. 284 – 287, 2019.

[22] M. A. Kadhim, H. S. Hamid, and N. R. Hadi, "Improvement of fixed WiMAX OSTBC-OFDM transceiver based wavelet signals by nonlinear precoding using SDR platform," *International Journal of Soft Computing and Engineering*, vol. 3, no. 5, pp. 143–150, 2013.

[23] S. G. Mallat, "A theory for multiresolution signal decomposition: the wavelet representation," *IEEE Transactions on Pattern Analysis and Machine Intelligence*, vol. 11, no. 7, pp. 674–693, 1989.

[24] A. Khan and S. Y. Shin, "Wavelet OFDM-based non-orthogonal multiple access downlink transceiver for future radio access," *IETE Technical Review*, vol. 35, no. 1, pp. 17–27, 2018.

[25] Y. Liu, M. P. Fitz, and O. Y. Takeshita, "A rank criterion for qam space-time codes," *IEEE Transactions on Information Theory*, vol. 48, no. 12, pp. 3062–3079, 2002.

[26] A. Khalid, "Wavelet transform based non-hermitian symmetry OFDM technique for indoor MIMO-VLC system with an imaging receiver," *Wireless Networks*, vol. 27, no. 7, pp. 4649–4663, 2021.

[27] J. W. Cooley and J. W. Tukey, "An algorithm for the machine calculation of complex Fourier series," *Mathematics of computation*, vol. 19, no. 90, pp. 297–301, 1965.